Civil and Environmental Engineering
Vol. 21, Issue 2, 864-876, DOI: 10.2478/cee-2025-0063

MODELLING TURBULENT KINETIC ENERGY AND STREAMLINES OVER GABION STEPPED WEIRS

Farah Hamid Al-MAJED[1], Mohammed A Almajeed A ALABAS[1,*]

[1] Department of Civil Engineering, Faculty of Engineering, University of Babylon, Babylon 51001, Iraq.
[*] Corresponding author: eng.mohammed.abidalabas@uobabylon.edu.iq

Abstract

Gabion weirs are environmentally friendly hydraulic structures that regulate floods and reduce bottom erosion by controlling flow velocity. This study aims to simulate the flow over gabion stepped weirs numerically. A three-dimensional simulation has been conducted using ANSYS Fluent software (ANSYS 2021 R1). A computational fluid dynamics (CFD) model utilizing the volume of fluid (VOF) technique with (Standard, RNG, and Realizable) k-Ɛ, and Standard k-ω turbulence models have been used. A laboratory-scale of gabion stepped model with a downstream slope of (1:1, 1:2, and 1:3 V: H), and porosity (0.42) was used to verify the numerical models, for three operational discharges (3.08E-3, 23.26E-3, and 52.63E-3) m^3/s. The downstream velocity was used to verify the numerical models. The results showed that all models agree with the experimental data. The root means square error (RMSE) values ranged between 0.14 and 0.309 and the determination of coefficient (R2) values ranged between 0.965 and 0.812, where the standard k-Ɛ model was the most representative of the flow condition and downstream velocity. The Turbulent Kinetic Energy (TKE) of a stepped gabion weir with a porosity of 0.42 and a slope of 1:2 was predicted. The results showed that the TKE values increased in the lower regions at the skimming flow regime, where the k-ω model showed the highest turbulence levels compared to the other models. Moreover, at the nappe flow regime, TKE peaks on the weir steps due to the generated eddies, while low discharges (through-flow regime) showed relatively stable flow. Furthermore, according to predicted streamlines, the porous medium reduces the flow velocity and the emergence of up-and-down flow at the weir crest. The effect of turbulence and seepage increases at high discharge, while turbulence decreases and flow lines become straighter at low discharge.

Keywords:

CFD;
Gabion stepped weir;
TKE;
Streamline;
Downstream velocity.

1 Introduction

Weirs are small structures used to raise the water level in rivers or streams, causing a noticeable change in the water level behind them. Spillways associated with dams are used in many engineering applications as safety devices, releasing excess water during floods to ensure the stability of the water system [1]. Gabion weirs are constructed by assembling stone-filled baskets to form the weir body, constituting the primary materials for gabion stepped weirs. Sediment and organic suspended material can easily pass through the weir body. Microorganisms in gabion weirs play a role in decomposing organic matter and purifying water while promoting water aeration through disturbances of air-water interfaces. Due to their limited environmental impact, gabion weirs are considered ecosystem-friendly. Hydrodynamic flow studies over stepped spillways show high velocities and aeration, influenced by step design and flow conditions, with remarkable agreement between experimental results and computational simulations [2]. The literature review focused on studying stepped spillways and developing basic equations related to design criteria. It addressed multiple flow regimes (nappe, transitional, and skimming) using stepped weirs in studies [3-5]. In addition, Peyras et al. [6] addressed the continuous flow regime. Laboratory experiments included research on flow characteristics and the effect of gabion-stepped weirs on energy dissipation, such as the works of Al-Fawzy et al. [7], Salmasi and Samadi [8], Mahjoubi and Kashefipour [9], and Zuhaira et al. [10]. The results showed that the weir discharge, porosity, and downstream slope directly affect the energy dissipation efficiency. Leu et al. [11], also highlighted the turbulent flow in rectangular wiers with different porosities (0.000, 0.349, and 0.475), which added a deeper understanding of the effect of porosity on flow dynamics. The results showed that the porous structures extend the recirculation area downstream due to the water flow passing through the gaps. In addition to the laboratory experiments, many numerical studies were used, where the computational fluid dynamics (CFD) method proved its popularity among researchers due to its time efficiency, low cost, and diverse applications in hydraulic models. Researchers adopted various geometric shapes of steps, sills, and chute angles to study the flow dynamics of stepped weirs and energy dissipation, as reported in the studies of Saleh and Hussein, Al-Hashemi et al.,[12]; Ghaderi et al., [13]; Hekmatzadeh et al.,[14]; Jahad et al.[15] and Ikinciogullari,[16], and Jahad et al., [17]. Recent studies have focused on the influence of various factors on flow dynamics and hydraulic structures using computational fluid dynamics (CFD). Muhsun and Al-Sharify [18]discussed the effect of longitudinal slope on the relationship between critical depth and central water depth above the weir. Tavakol-Sadrabadi et al., [19] and Soydan Oksal et al.,[20] used software such as FLUENT and ANSYS-FLUENT to study the flow behaviour over broad-crested and trapezoidal weirs, focusing on the effect of slope, particle diameters, and the accuracy of the Reynolds stress model (RSM). Daneshfaraz et al. [21] simulated the water flow through broad-crested weirs using FLOW-3D software, analysing turbulence models and flow velocities. In another study, Chan et al. [22] investigated the effect of rib design and porosity on the turbulent flow characteristics in channels, contributing to a deeper understanding of flow dynamics. Previous studies have highlighted the effect of flow and energy dissipation on weir dynamics. Salmasi and Samadi [23] used FLUENT software to study stepped spillways and concluded that flow rates affect energy dissipation and shear stress. In turn, Saadatnejadgharahassanlou et al. [24] and Boudjelal et al. [25] used computational fluid dynamics simulations to study flow over v-notch weirs and solid barriers, pointing out the importance of turbulence models and channel slopes in determining flow regimes. Imanian et al. [26] extended the research to broad-crested rectangular weirs, where they found a slight effect of head ratio on separation areas, with an efficient prediction of vortex formation using advanced turbulence models. Although many studies have addressed flow characteristics and different types of weirs, the information available on turbulence models for predicting complex flow around stepped gabion weirs remains limited. The present study simulates the flow over gabion stepped weirs with four turbulent models. The downstream velocity will be used to validate the model. It also aims to measure the turbulent kinetic energy generated along the weir steps and downstream, which helps understand the flow dynamics and its impact on weir design and operational effectiveness. This study highlights the role of computational fluid dynamics in optimising hydraulic designs and understanding flow behaviour across different weir configurations and operating conditions.

2 Methods

2.1 The Volume of Fluid (VOF)

The Volume of Fluid (VOF) method was used in computational fluid dynamics (CFD) for modelling multiphase flows. It was first developed in 1981 by Hirt and Nichols [27]. VOF is based on calculating the ratio of air to water at each point within a specified volume by measuring the volume ratio of each element in the space. Using these ratios, the air-water interface is determined by the continuity equation. VOF is one of the most effective methods for simulating multiphase flows [28].

2.2 The Numerical Model

The Navier-Stokes formulas and continuity equations are used by the ANSYS FLUENT program to control numerical modelling equations for turbulent (three-dimensional), incompressible flow across weirs. Newton's second law and mass conservation in the case of fluid movement serve as a basis for these equations. Differential equations [16] characterise these equations as follows:

$$\frac{\partial u}{\partial x}+\frac{\partial v}{\partial y}+\frac{\partial w}{\partial z}=0 \quad (1)$$

Navier–Stokes momentum equation:

Momentum in X-direction equation

$$\frac{\partial u}{\partial t}+u\frac{\partial u}{\partial x}+v\frac{\partial u}{\partial y}+w\frac{\partial u}{\partial z}=g_x-\frac{1}{\rho}\frac{\partial p}{\partial x}+\mu\left(\frac{\partial^2 u}{\partial x^2}+\frac{\partial^2 u}{\partial y^2}+\frac{\partial^2 u}{\partial z^2}\right) \quad (2)$$

Momentum in the Y-direction equation

$$\frac{\partial v}{\partial t}+u\frac{\partial v}{\partial x}+v\frac{\partial v}{\partial y}+w\frac{\partial v}{\partial z}=g_y-\frac{1}{\rho}\frac{\partial p}{\partial y}+\mu\left(\frac{\partial^2 v}{\partial x^2}+\frac{\partial^2 v}{\partial y^2}+\frac{\partial^2 v}{\partial z^2}\right) \quad (3)$$

Momentum in the Z-direction equation

$$\frac{\partial w}{\partial t}+u\frac{\partial w}{\partial x}+v\frac{\partial w}{\partial y}+w\frac{\partial w}{\partial z}=g_z-\frac{1}{\rho}\frac{\partial p}{\partial z}+\mu\left(\frac{\partial^2 w}{\partial x^2}+\frac{\partial^2 w}{\partial y^2}+\frac{\partial^2 w}{\partial z^2}\right) \quad (4)$$

where:
ρ: The fluid density; t: time; u, v, w: velocities in x, y, and z directions; p: the pressure; g: the gravity acceleration; μ: the fluid viscosity.

2.3 Turbulence Models

Turbulent flows are characterised by fluctuations in velocity fields that mix momentum, energy, and species concentration, causing continuous changes. Since direct simulation of these small fluctuations is difficult due to high computational cost [29] techniques such as time averaging or modification of the governing equations are used to reduce complexity. However, these modifications introduce additional unknown variables that are accounted for using turbulence models. In this study, four models were used to simulate the flow behaviour: the Standard k-Ɛ model, the RNG k-Ɛ model, the Realizable k-Ɛ model, and the Standard k-ω model as follows:

1-*Standard k-Ɛ Model*

The standard k-Ɛ model, introduced by Wilcox,[30] predicts turbulent flows by solving transport equations for turbulent kinetic energy (k) and its dissipation rate (Ɛ). While the equation for k is derived mathematically, the Ɛ equation is based on physical reasoning. This model assumes fully turbulent conditions, ignoring molecular viscosity, making it applicable only to such flows. As (Launder and Spalding, [31] the main governing equations include:

The turbulence kinetic energy, *k* Equation:

$$\frac{\partial}{\partial t}(\rho k) + \frac{\partial}{\partial x_i}(\rho k u_i) = \frac{\partial}{\partial x_j}\left[\left(\mu + \frac{\mu t}{\sigma_k}\right)\frac{\partial k}{\partial x_j}\right] + G_k + G_b - \rho_\varepsilon - Y_M + S_k \tag{5}$$

The turbulent Energy Dissipation Rate, Ɛ Equation:

$$\frac{\partial}{\partial t}\left(\rho\varepsilon\right) + \frac{\partial}{\partial x_i}\left(\rho\varepsilon u_i\right) = \frac{\partial}{\partial x_j}\left[\left(\mu + \frac{\mu_t}{\sigma_\varepsilon}\right)\frac{\partial \varepsilon}{\partial x_j}\right] + C_{1\varepsilon}\frac{\varepsilon}{k}(G_k + C_{3\varepsilon}G_b) - C_{2\varepsilon}\rho\frac{\varepsilon^2}{k} \quad + S_\varepsilon \tag{6}$$

The turbulent "eddy" viscosity, μ_t is calculated through an equation that relates the turbulent kinetic energy k to the turbulent energy dissipation rate $\mathcal{E}$.

$$\mu_t = \rho C_\mu \frac{k^2}{\varepsilon} \tag{7}$$

where the model constants $C_{1\varepsilon}$, $C_{2\varepsilon}$, C_μ, σ_k and σ_ε equal to 1.44, 1.92, 0.09, 1.0, and 1.3 respectively.

These equations deal with the production, transport, and dissipation of turbulent kinetic energy k and its dissipation rate Ɛ in incompressible flow. G_k expresses the energy produced by mean velocity gradients, G_b reflects buoyancy effects, and Y_M reflects the fluctuating expansion effect. Dissipation is controlled by the constants $C_{1\varepsilon}$, $C_{2\varepsilon}$, and $C_{3\varepsilon}$, and turbulent transport is affected by the Prandtl numbers σ_k and σ_ε. The equations also include source terms S_k and S_ε that are specific to specific flow conditions. The constant values are derived from experiments with turbulent shear flows in air and water, making them suitable for a wide range of free and steady shear flows near walls.

2- RNG k-ε Model

It is an advanced model for simulating fluid and gas turbulence, based on the Navier-Stokes equations using renormalisation theory (RNG). The model has higher accuracy than the standard k-Ɛ model for a wide variety of flows. [31].

The turbulence kinetic energy, *k* Equation

$$\frac{\partial}{\partial t}(\rho k) + \frac{\partial}{\partial x_i}(\rho k u_i) = \frac{\partial}{\partial x_j}\left(\alpha_k \mu_{eff}\frac{\partial k}{\partial x_j}\right) + G_k + G_b - \rho\varepsilon - Y_M + S_k \tag{8}$$

qThe turbulent Energy Dissipation Rate, Ɛ Equation

$$\frac{\partial}{\partial t}(\rho\varepsilon) + \frac{\partial}{\partial x_i}(\rho\varepsilon u_i) = \frac{\partial}{\partial x_j}\left(\alpha_\varepsilon \mu_{eff}\frac{\partial \varepsilon}{\partial x_j}\right) + C_{1\varepsilon}\frac{\varepsilon}{k}(G_k + C_{3\varepsilon}G_b) - C^*_{2\varepsilon}\rho\frac{\varepsilon^2}{k} \tag{9}$$

$$C_{2\varepsilon}^{*} \equiv C_{2\varepsilon} + \frac{C_{\mu}\eta^{3}(1-\eta/\eta_{o})}{1+\beta\eta^{3}} \tag{10}$$

where: the constants ($C_{1\varepsilon}$, $C_{2\varepsilon}$, C_m) equal to 1.42, 1.68, and 0.0845, respectively and (α_{ε}, α_k) equal to 1.393, η_0=4.38, μeff=1, β=0.012. Those values are used as default in ANSYS FLUENT.

3- *Realizable k-ε Model*

It is a popular model for describing the behaviour of turbulent fluids, as it satisfies the mathematical constraints of turbulent fluids. The model combines the Boussinesq relation with the determination of the eddy viscosity to obtain an expression for the Reynolds stress in incompressible turbulent flows [32].

$$\frac{\partial}{\partial t}(\rho k) + \frac{\partial}{\partial x_j}(\rho k u_j) = \frac{\partial}{\partial x_j}\left[\left(\mu + \frac{\mu_t}{\sigma_k}\right)\frac{\partial k}{\partial x_j}\right] + G_k + G_b - \rho\varepsilon - Y_M + S_k \tag{11}$$

$$\frac{\partial}{\partial t}(\rho \varepsilon) + \frac{\partial}{\partial x_j}(\rho \varepsilon u_j) = \frac{\partial}{\partial x_j}\left[\left(\mu + \frac{\mu_t}{\sigma_\varepsilon}\right)\frac{\partial \varepsilon}{\partial x_j}\right] + \rho C_1 S_\varepsilon - \rho C_2 \frac{\varepsilon^2}{k+\sqrt{v\varepsilon}} + C_{1\varepsilon}C_{3\varepsilon}G_b + S_\varepsilon \tag{12}$$

$$C_1 = max\left[0.43, \frac{\eta}{\eta+5}\right] \tag{13}$$

$$\eta = S\frac{k}{\varepsilon} \tag{14}$$

$$S = \sqrt{2S_{ij}}S_{ij} \tag{15}$$

$$S_{ij} = \frac{1}{2}\left(\frac{\partial u_j}{\partial x_i} + \frac{\partial u_i}{\partial x_j}\right) \tag{16}$$

where: $C_{1\varepsilon}$ =1.44, $C_{2\varepsilon}$ = 1.9, σ_k =1, σ_ε =1.2

4- *Standard k-ω Model*

The k-ω turbulence model is popular in computational fluid dynamics (CFD), first developed by Launder and Spalding [31]. This model adds two additional equations to the Navier-Stokes equations to describe the effects of turbulence, solving for the kinetic energy transfer k and its dissipation rate ω. Over time, production components have been added to improve the accuracy of predicting free shear flows according to [30].

The following transport equations represent:

The turbulent kinetic energy, k

$$\frac{\partial}{\partial t}(\rho k) + \frac{\partial}{\partial x_i}(\rho k u_i) = \frac{\partial}{\partial x_j}\left(\Gamma_k \frac{\partial k}{\partial x_j}\right) + G_k - Y_k + S_k \tag{17}$$

And, the specific dissipation rate, ω

$$\frac{\partial}{\partial t}(\rho \omega) + \frac{\partial}{\partial x_i}(\rho \omega u_i) = \frac{\partial}{\partial x_j}\left(\Gamma_\omega \frac{\partial \omega}{\partial x_j}\right) + G_\omega - Y_\omega + S_\omega \tag{18}$$

where:

G_k: Turbulence kinetic energy generation due to average velocity gradients,

G_ω: Generation of ω,

(Y_k, Y_ω): Dissipation of k and ω by turbulence,

(S_k, S_k): User-defined source variables,

(Γ_k, Γ_ω): Effective diffusivity of k and ω, respectively which is modelled as:

$$\Gamma_k = \mu + \frac{\mu_t}{\sigma_k} \tag{19}$$

$$\Gamma_\omega = \mu + \frac{\mu_t}{\sigma_\omega} \tag{20}$$

where:

(σ_k, σ_ω): Prandtl turbulence number of k and ω, respectively.

μ_t: Turbulent viscosity which combines k and ω, and computed as follows

$$\mu_t = \alpha^* \frac{\rho k}{\omega} \tag{21}$$

where:

α*: The impaired turbulent viscosity coefficient equal to 1

2.4 Boundary Conditions

The two-phase flow was simulated using the VOF method combined with the Forchheimer equation (1901) to represent the porous region in ANSYS FLUENT. To characterise the turbulent flow, the four turbulence models were used. The numerical model was operated at three different discharge rates (3.08E-3, 23.26E-3, and 52.63E-3) m^3/s. The upper stream inlet was divided into a water inlet and a pressure inlet, where the upper part was designated as a pressure inlet. At the same time, the lower outlet was a pressure outlet. The bottom, left, and right sides were treated as non-slip walls. The weir body was represented as a porous region. The boundary conditions included the flow velocity at the water inlet and the atmospheric pressure at the air inlet, with flow velocities of 0.011, 0.085, and 0.191 m/s based on the discharge rates. Details of the domain dimensions for the downstream slope 1:2 model are shown in Fig.1.

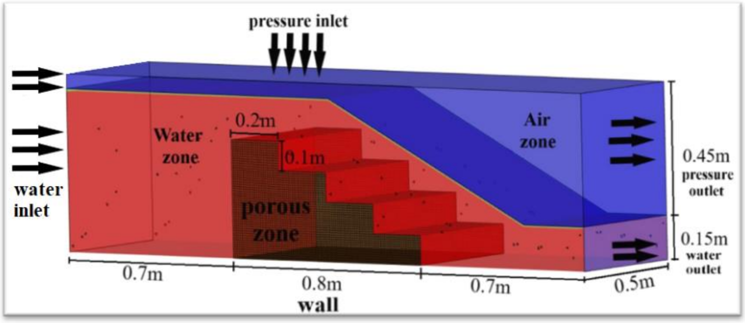

Fig. 1: Domain details.

2.5 Domain Description

The open channel flow domain consists of two main phases: water and air. A three-dimensional multiphase numerical model was used to simulate the flow in the channel using the VOF method to represent the contact interface between the two phases. The domain was divided into three main regions: water, air, and porous, as shown in Fig. 1. The water and porous regions were defined as the water phase in ANSYS FLUENT (R1, 2022) software, while the air region was considered the air phase. The mesh size is one of the significant factors for achieving high accuracy in the results [33,34]. Fine-structured meshes with an element size of 4 mm were used for both the water and pore regions, while the mesh in the air region was three times larger (12 mm) with 7549400 elements and 30787967 nodes for the k-ε model. Fig. 2 shows the details of the model mesh.

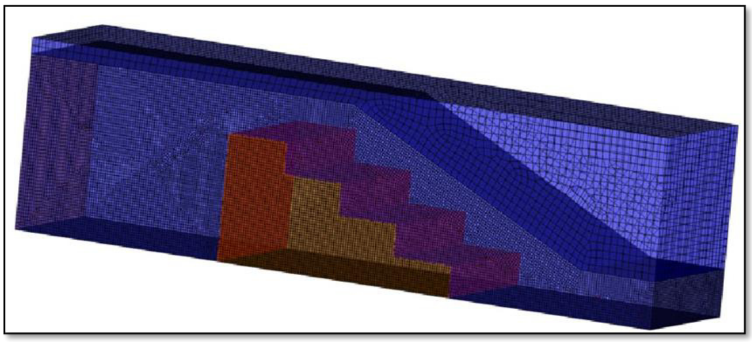

Fig. 2: Mesh details.

3 Results and Discussions

3.1 Validation CFD Model

The downstream flow velocity (V) is an important factor affecting the flow characteristics and energy dissipation rate. The downstream velocity of the stepped gabion weir (porosity 0.42) was selected to validate the numerical models based on the experimental data [35]. These datasets were used to evaluate the accuracy of the numerical model.

In the current study, a comparison was made between the downstream velocity of the experimental data and the numerical modelling results. This comparison is represented by the downstream velocity versus the drop number for the flow models across three slopes (1:1, 1:2, 1:3) and at three different operated discharges (3.08E-3, 23.26E-3, and 52.63E-3) m^3/s. Four turbulence models were used, the k-Ɛ (standard, RNG, Realizable) and the standard k-ω models. The root mean square error (RMSE) with the determination coefficient (R^2) (Eqs. 22 and 23) was used to evaluate the accuracy of the results obtained from the four numerical turbulent models and the experimental data.

$$RMSE = \sqrt{\frac{1}{n}\sum_1^n (O_{i\,Exp} - P_{i\,Num})^2} \quad (22)$$

$$R^2 = 1 - \frac{\sum_1^n (O_{i\,Exp} - P_{i\,Num})^2}{\sum_1^n (\bar{O}_{i\,Exp} - \bar{P}_{i\,Num})^2} \quad (23)$$

where: n is the number of results, O_{iExp}, P_{iNum} are depth values at point i for observed and predicted results, respectively, and $\bar{O}_{iExp}$, $\bar{P}_{iNum}$ indicate the corresponding mean values.

The numerical results generally agreed with the experimental data under all flow regimes for all turbulence models. The numerical models were applied under identical boundary conditions, material properties, mesh, etc. for all different turbulence models. In the case of the slope (1:1) as shown in Fig. 3, at the through-flow regime (lower discharge) corresponding to the drop number (0.00006), all turbulence models showed remarkable agreement with the experimental data. The numerical results were close to each other at the moderate and high discharge (napping and skimming) flow regimes corresponding to the drop numbers (0.00345, 0.01765), respectively. Still, they showed a slight divergence from the experimental data. However, these results indicate that the standard k-Ɛ model showed the highest level of agreement with the experimental data, indicating strong convergence. As confirmed by the statistical values of RMSE and R^2 (Table 1).

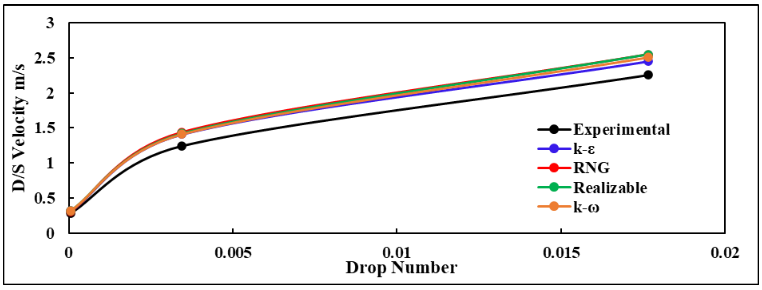

Fig. 3: Comparison of the downstream velocity between the experimental data and numerical models, for downstream slope 1:1.

Table 1: The root means square error (RMSE) and the determination coefficient (R^2) of four turbulent models with a downstream slope of 1:1.

The standard k-Ɛ		The RNG k-Ɛ		The Realizable k-Ɛ		The standard k-ω	
RMSE	**R^2**	**RMSE**	**R^2**	**RMSE**	**R^2**	**RMSE**	**R^2**
0.149112	0.965599	0.205242	0.934826	0.199637	0.938336	0.176918	0.951573

In the case of slope (1:2), there is a clear convergence between the numerical models and the experimental data, which was observed in the through-flow regime across the weir body. In contrast, in the case of the skimming flow regime, there is a slight divergence between the results of the numerical models and the experimental data. As for the case of the napping flow regime, the predicted downstream velocity for the turbulence models is shown in Fig. 4. The Realizable and standard k-Ɛ models showed the strongest agreement with the experimental data, according to values of RMSE and R^2 as shown in Table 2.

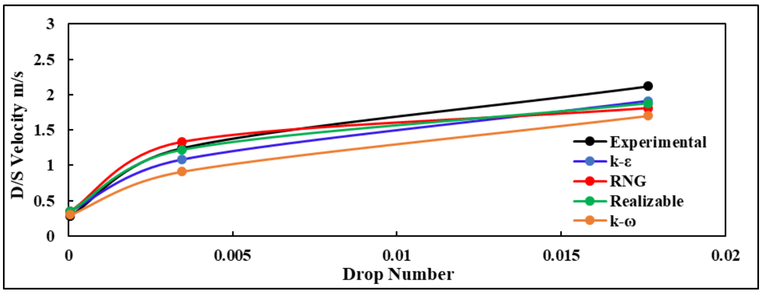

Fig. 4: Comparison of the downstream velocity between the experimental data and numerical models, for downstream slope 1:2.

Table 2: The root means square error (RMSE) and the determination coefficient (R^2) of four turbulent models with a downstream slope of 1:2.

The standard k-Ɛ		The RNG k-Ɛ		The Realizable k-Ɛ		The standard k-ω	
RMSE	R^2	RMSE	R^2	RMSE	R^2	RMSE	R^2
0.15828	0.955339	0.189875	0.935729	0.144474	0.96279	0.309562	0.829167

In the case of slope (1:3) Fig. 5, the numerical results showed a noticeable convergence with each other, to a greater extent than in the first slope (1:1). Although the four models were generally close to each other in the through flow regime across the weir body, some slight differences appeared in the napping and skimming flow regimes between the four turbulence models compared to the experimental data. The results indicated that the standard k-ω and the standard k-Ɛ models were the most consistent with the experimental data, as shown in Table 3.

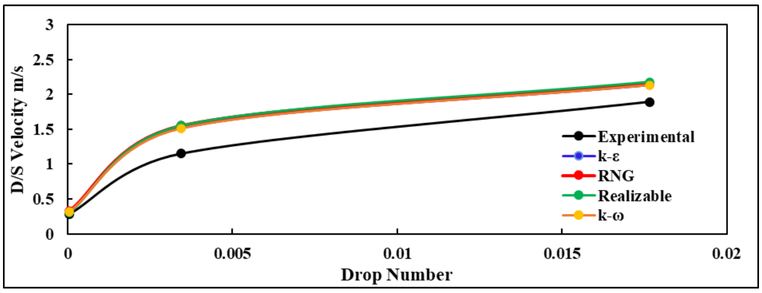

Fig.5: Comparison of the downstream velocity between the experimental data and numerical models, for downstream slope 1:3.

Table 3: The root means square error (RMSE) and the determination coefficient (R^2) of four turbulent models with a downstream slope of 1:3.

The standard k-Ɛ		The RNG k-Ɛ		The Realizable k-Ɛ		The standard k-ω	
RMSE	R^2	RMSE	R^2	RMSE	R^2	RMSE	R^2
0.258076	0.845547	0.275748	0.823671	0.284509	0.812289	0.249653	0.855465

The effect of the slope on the downstream horizontal velocity value can be observed, as the flow velocity increases with the increasing steepness of the slope, especially at the skimming flow regime (Q=52.63E-3 m^3/s) in the slope (1:1). For all of the turbulence models, the velocities were higher compared to slopes (1:2) and (1:3) under the same operative discharge. Increased horizontal velocity downstream leads to increases in the turbulence kinetic energy for the same direction, enhancing the turbulent flow of dynamics. As a result, the standard k-Ɛ model was the most representative of the flow condition and downstream velocity. This was inferred from the statistical values, as the model was the most and closest to the experimental data.

3.2 Turbulent Kinetic Energy (TKE)

TKE is a fundamental characteristic that occurs in the velocity gradient over spillways [36]. Numerous studies of spillways with different discharges have shown that TKE fluctuations follow a similar pattern. It is also an important indicator of the chaotic and unpredictable motion of water molecules during turbulent flow [37], the same as over spillways. TKE accounts for the exchange of energy between different points within the system and is a vital factor in understanding the mean velocity gradients that contribute to its emergence. This concept is important in hydrodynamics as it affects many aspects of turbulent flow. Therefore, measuring TKE intensity is useful for modelling the behaviour of systems under different turbulent flow conditions.

The ANSYS Fluent software was used to calculate the turbulent kinetic energy (TKE) of a gabion-stepped weir with a porosity of 0.42 and a slope of 1:2, under the influence of three operational discharges (3.08E-3, 23.26E-3, and 52.63E-3) m^3/s and four turbulence models (standard, RNG, Realizable) k-Ɛ and Standard k-ω. It was found that the higher discharge increased the downstream TKE values.

In the skimming flow regime at high discharge (Q = 52.63E-3 m^3/s), the stepped gabion weirs were treated as non-stepped solid weirs due to the discharge intensity. The TKE variation results showed significant variation between the models, highlighting the effect of model selection on the TKE values. The standard k-ω model, Fig. (6-d), showed the highest turbulence level, especially in the downstream region, which is noticeable at the lower steps due to the discharge intensity. This was followed by the standard k-Ɛ model, Fig. (6-a), which showed moderate turbulence at the lower steps and high turbulence intensity in the downstream region away from the steps. The other models (RNG and Realizable), Figs. (6-b and 6-c) showed relatively low turbulence in the lower steps and the downstream region as shown in Fig. 7.

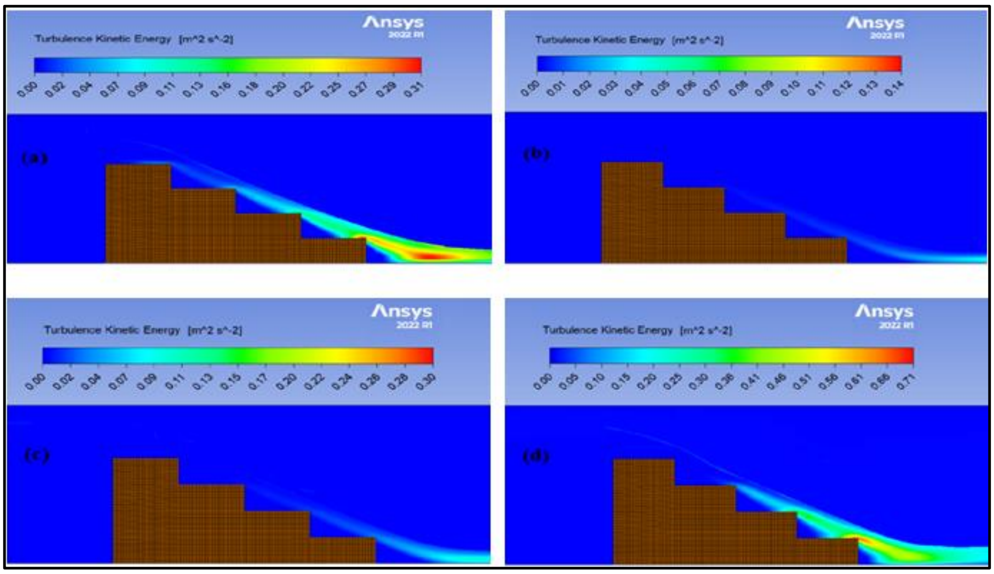

Fig. 6: Predicted TKE in slope 1:2 with operation discharge (Q=52.63E-3 m^3/s) and four turbulence models: (a) the standard k-Ɛ, (b) the RNG k-Ɛ, (c) the Realizable k-Ɛ, (d) the standard k-ω.

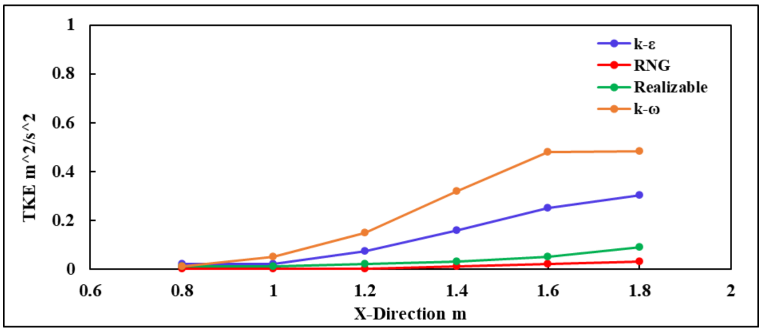

Fig.7: The max TKE on spillway with slope1:2 for operation discharge (Q=52.63E-3 m^3/s) and four turbulence models (standard, RNG, Realizable) k-Ɛ, and Standard k-ω.

The highest TKE values were observed at the middle discharge (Q=23.26E-3 m^3/s) along the spillway steps, which is what most turbulence models have shown. This is in the case of turbulent napping flow, which is a series of successive movements falling regularly on the spillway steps (Chanson et al., [22]. The flow velocity is lower than in skimming flow, but it is large enough to form a munt of vortices, which leads to an increase in the kinetic energy and the depth of the water at the outer edge of the steps. This flow region shows high turbulence, which reveals the occurrence of hydraulic jumps mainly formed there. This flow pattern above the steps is characterised by a change from subcritical to supercritical flow due to falling off, and from supercritical to subcritical flow due to the hydraulic jump [38]. Turbulence develops and spreads in the entire flow region, and water particles follow irregular paths that may not be continuous [39]. This is what the turbulence models showed, where the standard k-ω model, Fig. (8-d), showed the highest turbulence intensity compared to the other models, with the value gradually increasing along the stepped spillway. The standard k-Ɛ model, Fig. (8-a), observed a noticeable increase in turbulence intensity along the spillway steps, reaching its maximum intensity at the last step, but at a minimum rate than the case of the k-ω. The other models, (RNG and Realizable), Figs. (8-b, 8-c), showed relatively lower turbulence intensity than k-Ɛ, k-ω.

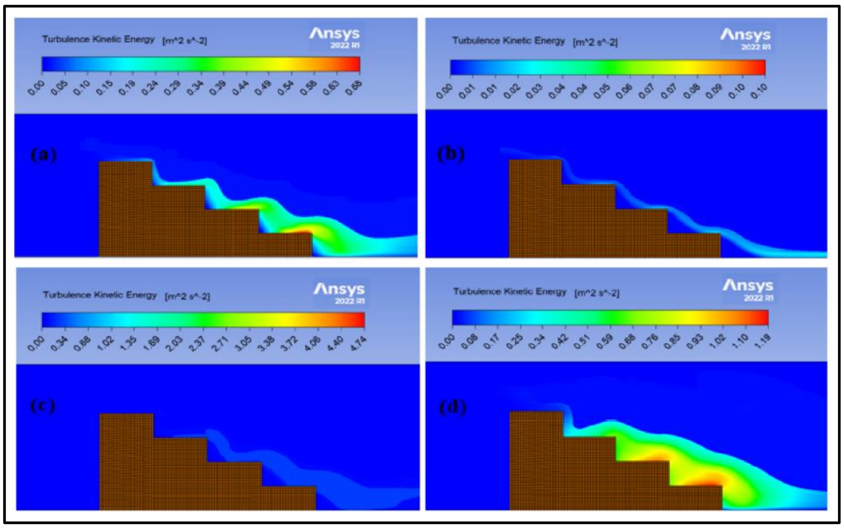

Fig. 8: Predicted TKE in slope 1:2 with operation discharge (Q=23.26E-3 m^3/s) and four turbulence models: (a) the standard k-Ɛ, (b) the RNG k-Ɛ, (c) the Realizable k-Ɛ, (d) the standard k-ω.

Referring to Fig. 9, we note that the TKE on the steps is higher than the TKE in U/S or D/S. This is due to the flow behaviour in the nape flow on the steps, which was explained previously.

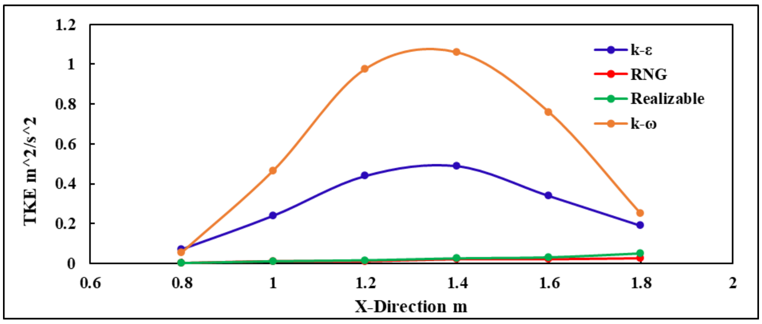

Fig. 9: The max TKE on spillway with slope1:2 for operation discharge (Q=23.26E-3 m^3/s) and four turbulence models (Standard, RNG, Realizable) k-Ɛ, and Standard k-ω.

When low-discharge (Q=3.08E-3 m^3/s) flow occurs within a gabion weir, it remains calm and stable. This is due to the shallow depth of the flow, which keeps it away from the spillway surface, reducing the possibility of significant turbulence. However, slight and imperceptible turbulence may be observed downstream, which does not significantly affect the stability of the flow. This was observed in all turbulence models as shown in Fig.10.

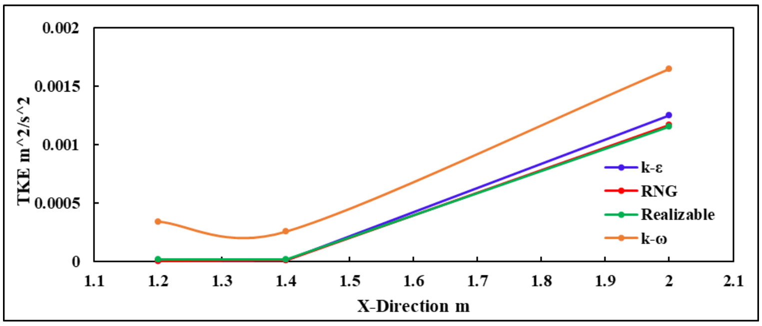

Fig.10: The max TKE on spillway with slope1:2 for operation discharge (Q=3.08E-3 m^3/s) and four turbulence models (Standard, RNG, Realizable) k-Ɛ, and Standard k-ω.

It has been noted from the above that each turbulence model uses different equations to estimate the generation and dissipation of turbulent kinetic energy. These differences in equations lead to differences in the distribution of TKE in the computational domain. Turbulence models also have empirical constants tuned to suit particular types of flows [31]. Variations in these constants greatly affect simulation results, especially in complex regions such as the downstream region. Each model is based on a set of assumptions about the nature of the turbulence. These assumptions may be more appropriate for certain types of flows than for others. Differences in these constants greatly affect the simulation results, especially in complex regions such as the downstream region and on steps. Each model relies on a set of assumptions about the nature of the turbulence. These assumptions may be more appropriate for certain types of flows than others. In the case of the different flow regimes above, the k-ω model was found to have results within estimation for TKE distribution in general flows, the standard k-Ɛ model is considered more accurate in near-wall regions [30].and therefore its results are above estimations, while the rest of the models (RNG, Realizable) had results under estimations. This indicates that there is agreement with the validation in the downstream velocity of the models with experimental data.

3.3 Streamlines and The Flow Behaviour

Studying streamlines can provide a better understanding of flow patterns on stepped gabion weirs. It is not easy to predict flow over and through porous media without numerical models that examine porous media with different flow rates. The flow behaviour around the stepped gabion weir (1:2 downstream slope) was analysed using the standard k-Ɛ turbulence model with three flow regimes (skimming flow, nappe flow, and through flow) according to the amount of discharge (Q_1=52.63E-3 m^3/s, Q_2=23.26E-3 m^3/s, and Q_3=3.08E-3 m^3/s) respectively.

Fig.11 shows the Streamlines around a weir with a porosity of 0.42. Results of the numerical model indicate that flow patterns and velocity directions around the weir body are influenced by the porosity media, as gabion weirs allow water to flow into the porous medium, which leads to a reduction in velocity over the structure. Part of the approaching water flows through gaps in the porous weir and continues moving downstream.

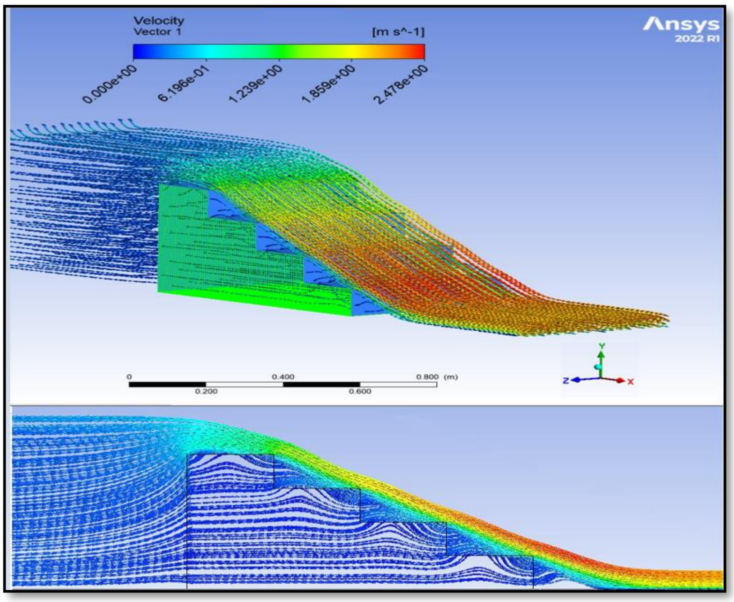

Fig. 11: The streamlines of velocity vectors for the standard k-Ɛ turbulence model for a stepped gabion weir at *(Q_1=52.63E-3) m^3/s.*

The results indicate that a portion of the flow entering the porous domain of the weir, especially at the weir's front, moves upward, exits from the beginning of the weir's crest and re-enters the porous media from the end of the crest. This phenomenon results from resistance to the flow of porous media and the formation of a low-pressure zone at the weir's crest due to the high velocity of the flood, as presented in Fig. 11.

Water flows from the high-pressure zone (low-velocity) of the porous media to the low-pressure zone (high-velocity) of the overflow, potentially leading to upward flow at the first part of the weir's crest and downward flow at the second part. This behaviour effectively explains the pressure distribution within the porous body (mentioned above), which agrees well with the findings of [40].

Excess flow pushes upwards, preventing overflow from entering the porous media. a condition that occurs at every step of the weir downstream, as the water rises at the beginning of each step and enters the weir body at its end. This phenomenon generally decreases with the reduction in flow velocity over the weir Fig. 12, with the flow curves remaining close to the horizontal surface of the steps within the porous medium. In addition, the depth of flow over the steps was greater at the lower steps than in the upper steps due to increased flow seepage across the vertical face of the lower steps.

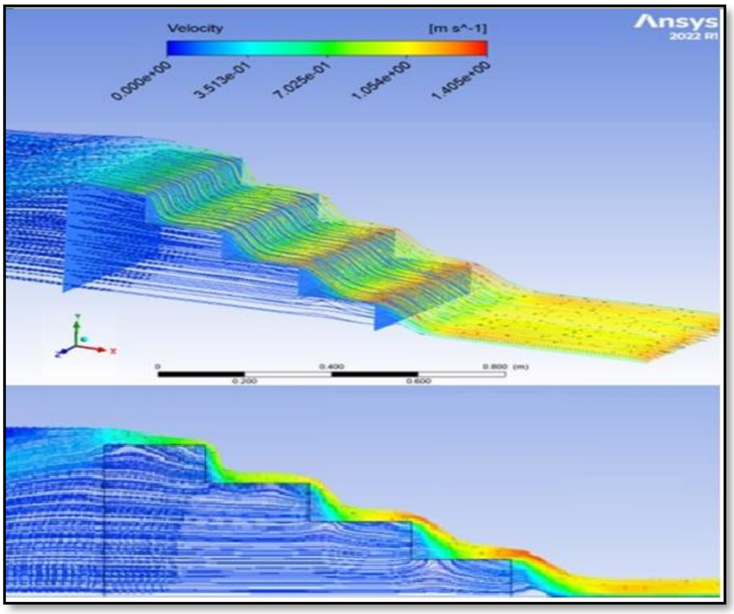

Fig. 12: The streamlines of velocity vectors for the standard k-Ɛ turbulence model for a stepped gabion weir at *(Q_2=23.26E-3) m³/s.*

At low velocities, Fig. 13, flow lines are in an almost straight curve, with the water depth downstream being much less than the water depth upstream. The water enters the porous medium and exits through the vertical face of the last step. It can be observed that the flow lines for all flow regimes appear parallel and horizontal within the weir body, except near the steps, which is due to the occurrence of turbulent flow at the surface. This may be due to the similar characteristics of the porous media.

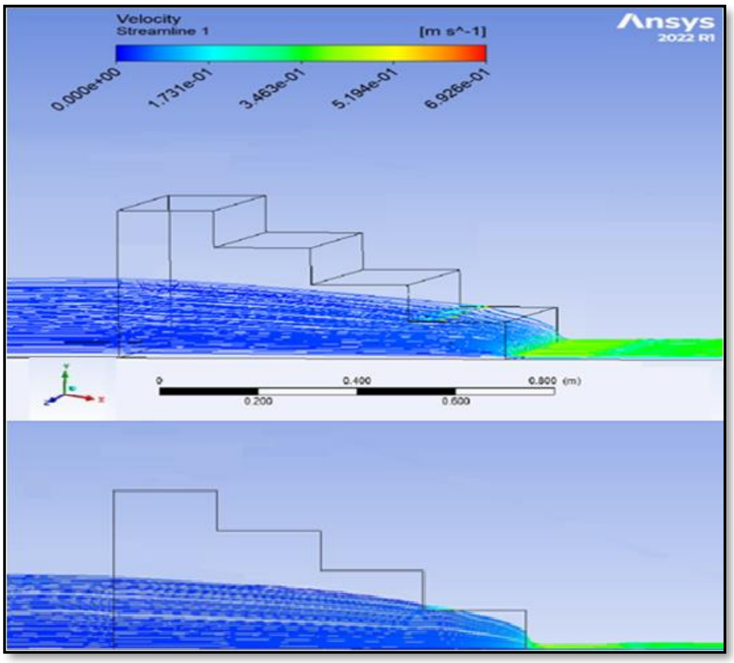

Fig. 13: The streamlines of velocity vectors for the standard k-Ɛ turbulence model for a stepped gabion weir at *(Q_3=3.08E-3) m^3/s.*

4 Conclusion

Gabion weirs are environmentally friendly hydraulic structures that regulate floods and reduce bottom erosion by controlling flow velocity. The research presented a numerical simulation of flow over gabion stepped weirs with different turbulent models. Results indicated that the numerical values of downstream velocity showed a good agreement with the experimental data across all turbulence models. According to the values of RMSE and R^2, the standard k-Ɛ model was the most representative of the flow condition and downstream velocity. Moreover, the study showed that the intensity of TKE depends on the flow regime (the amount of discharge). At the skimming flow regime (high discharge), the standard k-ω model shows the highest turbulence intensity, while other models, such as the standard k-Ɛ, show relatively less turbulence. At the nappe flow regime (medium discharge), TKE peaks on the weir steps due to the generated eddies, while the flow is stable at low discharge. The analysis of the streamlines around stepped gabion weirs shows the effect of porous media and discharge on the flow velocity and pressure distribution. The porous medium contributes to reducing the flow velocity and the emergence of up-and-down flow at the weir crest. The effect of turbulence and seepage increases at high discharge, while turbulence decreases, and flow lines become straighter at low discharge. According to the results, the k-Ɛ model is recommended for simulating the flow over gabion weirs. More studies may be needed on the effect of a wider range of porosity.

References

[1] LV, X.- ZOU, Q. - REEVE, D.: Numerical simulation of overflow at vertical weirs using a hybrid level set/VOF method. 2011. Advances in Water Resources, 34(10), pp.1320–1334.
[2] JAHAD, U.- AL-AMERI, R. - DAS, S.: Investigations of velocity and pressure fluctuations over a stepped spillway with new step configuration. 2022. Water Supply, 22(7), pp.6321–6337.
[3] SALMASI, F. - ÖZGER, M.: Neuro-fuzzy approach for estimating energy dissipation in skimming flow over stepped spillways. 2014. Arabian Journal for Science and Engineering, 39, pp.6099–6108.
[4] AL-MOHAMMED, F.- MOHAMMED, S.: Flow through and over gravel gabion weirs. 2015. Journal of Kerbala University, 13(25), pp.193-205.
[5] CHAMANI, M.- RAJARATNAM, N.: Characteristics of skimming flow over stepped spillways. 1999. *Journal of Hydraulic Engineering*, *125*(4), pp.361-368.
[6] PEYRAS, L.- ROYET, P. - DEGOUTTE, G.: Flow and energy dissipation over stepped gabion weirs. 1992. Journal of Hydraulic Engineering, 118(5), pp.707–717.
[7] AL-FAWZY, A.- AL-MOHAMMED, F.- AL-FATLAWI, T.- AL-ZUBAIDY, R.: Dissipation energy of flow by stepped type gabion weir. 2020, February. In IOP Conference Series: Materials Science and Engineering (Vol. 737, No. 1, p. 012158). Iop Publishing.
[8] SALMASI, F. - SAMADI, A.: Experimental and numerical simulation of flow over stepped spillways. 2018. Applied Water Science, 8(8), p.229.
[9] MAHJOUBI, F. - KASHEFIPOUR, S.: Investigation the energy dissipation on gabion stepped weirs and downstream hydraulic jump characteristics. 2023. Irrigation Sciences and Engineering, 46(1), pp.65–76.
[10] ZUHAIRA, A.- AL-HAMD, R.- ALZABEEBEE, S. - CUNNINGHAM, L.: Numerical investigation of skimming flow characteristics over non-uniform gabion-stepped spillways. 2021. *Innovative Infrastructure Solutions*, 6, pp.1–19.
[11] LEU, J.- CHAN, H.- CHU, M.: Comparison of turbulent flow over solid and porous structures mounted on the bottom of a rectangular channel. 2008. Flow Measurement and Instrumentation, 19(6), pp.331–337.
[12] AL-HASHIMI, S.- MADHLOOM, H.- NAHI, T.: Experimental and numerical simulation of flow over broad crested weir and stepped weir using different turbulence models. 2017. Journal of Engineering and Sustainable Development, 21(2), pp.28-45.
[13] GHADERI, A.- ABBASI, S. - DI FRANCESCO, S.: Numerical study on the hydraulic properties of flow over different pooled stepped spillways. 2021. Water, 13(5), p.710.
[14] HEKMATZADEH, A.- PAPARI, S. - AMIRI, S.: Investigation of energy dissipation on various configurations of stepped spillways considering several RANS turbulence models. 2018.Iranian Journal of Science and Technology, Transactions of Civil Engineering, 42, pp.97–109.
[15] JAHAD, U.- CHABUK, A.- ALABAS, M.- MAHMOUD, A.- AL-ANSARI, N. - LAUE, J.: CFD analysis of the effects of compound downstream slope on flow over the spillway. 2023. *Journal of Ecological Engineering*, 24(11), pp.274–286.
[16] IKINCIOGULLARI, E.: Stepped spillway design for energy dissipation. 2023.Water Supply, 23(2), pp.749–763.

[17] JAHAD, U.- CHABUK, A.- ALABAS, M.- MAHMOUD, A.- AL-ANSARI, N. - LAUE, J.: CFD analysis of the effects of compound downstream slope on flow over the spillway. 2023. Journal of Ecological Engineering, 24(11), pp.274–286.
[18] MUHSUN, S.- AL-SHARIFY, Z.: CFD simulated model and experimental tests for critical depth and flowrate estimation over a broad-crested weir under the longitudinal slope effect. 2021.International Journal of Environment and Waste Management, 28(1), pp.41–60.
[19] TAVAKOL-SADRABADI, M.- FATHI-MOGHADDAM, M.- MOHAMMADPOUR, R.: Numerical simulation of the over and through flow discharge in broad-crested gabion weirs with side slopes. 2018. Amirkabir Journal of Civil Engineering, 50(4), pp.619–630.
[20] SOYDAN OKSAL, N.- AKOZ, M.- SIMSEK, O.: Numerical modelling of trapezoidal weir flow with RANS, LES and DES models.2020 *Sādhanā*, 45(1), p.91.
[21] DANESHFARAZ, R.- BAGHERZADEH, M.- GHADERI, A.- DI FRANCESCO, S. - ASL, M.: Experimental investigation of gabion inclined drops as a sustainable solution for hydraulic energy loss. 2021. Ain Shams Engineering Journal, 12(4), pp.3451-3459.
[22] CHANSON, H. - GUALTIERI, C.: Similitude and scale effects of air entrainment in hydraulic jumps. 2008. Journal of Hydraulic Research, 46(1), pp.35-44.
[23] SALMASI, F. - SAMADI, A.: Experimental and numerical simulation of flow over stepped spillways. 2018. *Applied Water Science*, 8(8), p.229.
[24] SAADATNEJADGHARAHASSANLOU, H.- ZEYNALI, R.- GHAREHBAGHI, A.- MEHDIZADEH, S. - VAHEDDOOST, B.: Three dimensional flow simulation over a sharp-crested V-Notch weir. 2020. Flow Measurement and Instrumentation, 71, p.101684.
[25] BOUDJELAL, S.- FOURAR, A. - MASSOUH, F.: Experimental and numerical simulation of free surface flow over an obstacle on a sloped channel. 2022. Modeling Earth Systems and Environment, 8(1), pp.1025-1033.
[26] IMANIAN, H.- MOHAMMADIAN, A. - HOSHYAR, P.: Experimental and numerical study of flow over a broad-crested weir under different hydraulic head ratios. 2021. Flow Measurement and Instrumentation, 80, p.102004.
[27] JAHAD, U.- CHABUK, A.- AL-AMERI, R.- MAJDI, H.- MAJDI, A.- AL-ANSARI, N.- ABED, S.: Flow characteristics and energy dissipation over stepped spillway with various step geometries: case study (steps with curve end sill). 2024. Applied Water Science, 14(3), p.60.
[28] HIRT, C.- NICHOLS, B.: Volume of fluid (VOF) method for the dynamics of free boundaries. (1981). Journal of computational physics, 39(1), 201-225.
[29] TENNEKES, H.- LUMLEY, J.: A first course in turbulence. 1972. MIT Press.
[30] WILCOX, D.: Turbulence modeling for CFD. 1998. DCW Industries, La Canada.
[31] LAUNDER, B.- SPALDING, D.: The numerical computation of turbulent flows. In: *Numerical Prediction of Flow, Heat Transfer, Turbulence and Combustion*. 1983. Pergamon, pp.96–116.
[32] YAKHOT, V. - ORSZAG, S.: Renormalization group analysis of turbulence. I. Basic theory. 1986. Journal of Scientific Computing, 1(1), pp.3–51.
[33] AL SHAIKHLI, H. - MOHAMMED, S. - AL-KHAFAJI, Z.: Using Flow 3D Simulation, Multiple Nonlinear Regression Approach, and Artificial Neural Network Approach Approaches to Study the Behavior of Vertical Drop Structures. Civil and Environmental Engineering, 20.2, 2024, pp. 654-683.
[34] DAKHEEL, A. - ISMAEEL, A. - MAKKI, J.: Numerical modelling of local scour depth at non-uniform piers. 2024. Civil and Environmental Engineering, 20.2, 2024, pp. 699-710.
[35] ALABAS, A. -ALMAJEED, M.-.: Investigation of Flow Characteristics and Energy Dissipation in Gabion Stepped Weirs 2020 (Doctoral dissertation, Deakin University).
[36] BOMBARDELLI, F.- MEIRELES, I.- MATOS, J.: Laboratory measurements and multi-block numerical simulations of the mean flow and turbulence in the non-aerated skimming flow region of steep stepped spillways. 2011. Environmental fluid mechanics, 11(3), pp.263-288.
[37] POPE, S.: Turbulent flows. 2001. *Measurement Science and Technology*, *12*(11), 2020-2021.
[38] JALIL, S.- QASIM, J.- JALIL, S.: Numerical modelling of flow over single-step broad-crested weir using FLOW-3D and HEC-RAS. 2016. Polytechnic General Sciences Journal, Erbil Polytechnic University, 6, pp.435–448.
[39] CHANSON, H.: Hydraulics of open channel flow. 2004. Elsevier.
[40] FATHI-MOGHADDAM, M.- SADRABADI, M.- RAHMANSHAHI, M.: Numerical simulation of the hydraulic performance of triangular and trapezoidal gabion weirs in free flow condition. 2018. Flow Measurement and Instrumentation, 62, pp.93–104.